Theor Chem Acc (1998) 100:12–20
DOI 10.1007/s002149800m55

Theoretical
Chemistry Accounts

Regular article

The unrestricted natural orbital-restricted active space method: methodology and implementation*

Pawel M. Kozlowski, Peter Pulay**

Department of Chemistry, University of Arkansas, Fayetteville, AR 72701, USA

Received: 16 July 1998 / Accepted: 7 August 1998 / Published online: 19 October 1998

Abstract. The full configuration interaction method in the space of fractionally occupied unrestricted natural orbitals (UNO-CAS method) is extended to excited states as well as to strongly correlated and reactive systems with large active spaces. This is accomplished by using restricted active space (RAS) wave functions introduced by Olsen et al. [(1988) J Chem Phys 89: 2185] and using the UNOs without the expensive orbital optimization step. In RAS, the space of active orbitals is subdivided into three groups: a group with essentially doubly occupied orbitals (RAS1), the usual CAS space (RAS2), and a space with weakly occupied active orbitals (RAS3). We select these spaces on the basis of the occupation numbers of the UNOs. All possible electron distributions are allowed in the usual CAS space, but the number of vacancies is limited in RAS1 and the number of electrons is limited in RAS3. We discuss an efficient algorithm for generating a RAS wave function. This is based on the Handy-Knowles determinantal expansion with an addressing scheme adopted for the restricted expansion. Results for both ground and excited states of azulene and free base porphyrin are presented.

Key words: Restricted active space – Unrestricted natural orbitals – CI

1 Introduction

The complete active space (CAS) wave function is usually an excellent zeroth-order description for reactive potential surfaces. In the CAS approach the orbital space is partitioned into a space of doubly occupied orbitals, an active space, and a virtual space. The CAS wave function is a linear combination of configurations resulting from all possible electron distributions in the active space. In the CAS-SCF optimization procedure both the configuration interaction (CI) coefficients and the orbitals are optimized until the energy becomes stationary (see the review articles by Werner, Shepard and Roos in Ref. [1]). The computational cost of this procedure grows enormously with the dimension of the active space, and current hardware limits the active space to about 12 orbitals (larger if symmetry can be used). The cost of CAS calculations is determined by two factors. For smaller active spaces the optimization of the active orbitals is dominant; for larger active spaces the solution of the secular equation is the most time-consuming part. Another drawback of the CAS method is the arbitrariness in the selection of the active orbitals, particularly for large molecules, where chemical intuition often does not suffice. In our opinion, the active space should include only orbitals required for the correct description of the nondynamical (static or quasi-degenerate) correlation. The inclusion in the active space of orbitals which do not participate in strong electron correlation usually leads to an unbalanced treatment of nondynamical and dynamical correlation effects. The effect of the former can be included in other ways, for example using multireference second-order perturbation theory [2–4].

In the present study we focus on the cost-effective calculation of nondynamical correlation effects. An inexpensive alternative to the CAS-SCF method based on full configuration inter-action in the space of fractionally occupied unrestricted Hartree-Fock natural orbitals (UNOs) has been proposed by Pulay and coworkers; this is known as the unrestricted natural orbital-complete active space (UNO-CAS) method [5]. This method is based on the observation that the natural orbitals of the unrestricted Hartree-Fock (UHF) wave function are good approximations to the CAS-SCF orbitals [6]. In most cases, this method requires only a fraction of the computational effort in comparison to CAS-SCF and gives comparable results (see, e.g., recent results for the phenoxy radical [7]). Gradient formulation is more

*Dedicated to Prof. Dr. Wilfried Meyer on the occasion of his 60th birthday

**Present address*: Department of Chemistry, Princeton University, Princeton, NJ 08544, USA

Correspondence to: P. Pulay

complex due to the fact that orbitals are not optimized; however from a computational point of view, gradient evaluation is not significantly more expensive than for the CAS-SCF method [5, 8]. The UNO-CAS technique has been applied to many different problems, for example the McLafferty rearrangement [9], the identification of the $C_3 + H_2O$ reaction product [10], the hexatriynyl radical [11], the vibrational spectroscopy of *p*-benzoquinone [12], the geometries of conjugated π systems [13], and the vibrational spectrum of the phenoxy radical [7]. An advantage of the UNO-CAS method compared to CAS-SCF is that the active space is automatically determined by the occupation numbers of the UNOs. The usual criterion is to include orbitals in the active space if the occupation is between 0.02 and 1.98 (this follows from the correlation between UHF NO occupancy and nondynamical correlation [6]). A disadvantage of the UNO-CAS (and UNO-RAS) treatment compared to CAS-SCF is that, with rigid thresholds on the occupation numbers, the active space can change suddenly, resulting in steps on the energy surface. Addition of dynamical correlation diminishes these artifacts but does not fully remove them. They can be removed by switching to CAS-SCF, for which UNO-CAS can provide excellent starting orbitals, or using the NOs of the half-projected Hartree-Fock method [14].

The aim of the present study is twofold. All previous applications of the UNO-CAS method have been restricted to ground state energies and properties; here we present an extension of the UNO-CAS method to excited states. Additionally, we apply the method to strongly correlated and reactive systems with large active spaces (i.e., with more than 12 active orbitals). For example, free base porphyrin contains 18 UHF NOs with significant fractional occupation, including four very strongly correlated orbitals (see next section). At this moment it is technically not feasible to consider 18 orbitals and 18 electrons in a CAS expansion. A convenient solution to this problem was suggested by Olsen et al. [15] by using a restricted active space (RAS) wave function. For a RAS wave function the space of active orbitals is subdivided into three groups of orbitals denoted by RAS1, RAS2, and RAS3, respectively. The RAS1 space consists of orbitals which are more-or-less doubly occupied and only a limited number of holes, usually 2, is allowed. RAS3 contains a set of weakly occupied active orbitals and only a limited number of electrons, in most cases 2, is permitted. RAS2 corresponds to the usual CAS active space with all possible electron distributions allowed. This approach reduces the length of the expansion significantly; however it is no longer size-consistent. Another weakness of the original RAS methodology is that it lacks a unique definition of the RAS spaces and relies on chemical intuition. In the UNO-RAS method the RAS spaces can be automatically determined based on the occupation of UNO orbitals. For instance, a reasonable set of criteria is to include UNOs with occupation between 1.90 and 1.98 in RAS1, between 0.1 and 1.9 in RAS2, and between 0.02 and 0.1 in RAS3. In the free base porphyrin case, this gives a $7+4+7$ RAS wave function, which is quite feasible to calculate.

The organization of the paper is as follows. First we show how to generate the CI space for a RAS expansion. To accomplish this we use the determinantal approach of Handy and Knowles [16]. Since the RAS expansion is usually large, solution of the secular equation is the dominant part of the calculation. We then discuss the computational implementation of the UNO-RAS method, in particular the direct construction of the sigma vector, $\sigma = \mathbf{Hc}$, from molecular integrals and the trial vector $\mathbf{c}$. The final section contains preliminary results for ground and excited states of azulene and free base porphyrin.

2 CI space generation for RAS

Knowles and Handy [16] realized that a CI expansion based on determinants, rather than spin-adapted configuration state functions, can be constructed without a precomputed list of coupling coefficients. Since this earlier work, many different variants of the Knowles-Handy algorithm have appeared in the literature [17–27]. The most representative applications of these techniques are the benchmark CI calculations of Bauschlicher et al. [21] and the billion CI determinantal expansion of Olsen et al. [22]. The main idea of determinant-based CI is to deal separately with the alpha and beta spinorbitals. Although this approach sacrifies part of the spin symmetry, it reduces the configuration list enormously by allowing it to be written as a direct product of an α and a β occupancy. Occupancies are stored in form of strings, I_α and I_β, which are ordered products of creation operators. Denoting the number of α and β electrons in the active space by N_α and N_β, and the number of active orbitals by n, there are $\binom{n}{N_\alpha}$ possible alpha strings and $\binom{n}{N_\beta}$ beta strings, respectively. Following Knowles and Handy [16], lexical order can be introduced for strings and the address associated with the string (Addr $\{I_\alpha\}$ for alpha strings and Addr $\{I_\beta\}$ for beta strings, respectively). Thus, the CI expansion can be constructed as a sequence of mappings between strings and molecular integrals.

Apart from the work of Olsen et al. [15] relatively little attention has been paid to the development of restricted schemes where not all possible excitations are allowed in the active space. In the next part of this section we describe a simple scheme for generating a RAS expansion. Extension of this scheme to Abelian point group symmetry is straightforward, and we do not discuss it here. In practice, any alpha (or beta) string can be generated as a list of occupied orbital indices, $\{\phi_i;\ i = 1, 2, \ldots N\}$ in ascending order. (Note that ϕ_i is the index of the orbital, not the orbital itself.) For example, in the case of $n = 5$ orbitals and $N = 3$ electrons one can generate ten alpha strings: (123), (124), (134), (234), (125), (135), (235), (145), (245), (345). For string generation we used reverse lexical ordering according to the terminology of Duch [23]. In order to visualize the CI space generated by the strings a graphical representation can be used. Duch [28] describes this in detail. For reverse lexical ordering, the address of string I is given by

$$\mathrm{Addr}\{I\} = 1 + \sum_{i=1}^{N} \binom{\phi_i - 1}{i} \ . \tag{1}$$

Suppose we would like to construct a RAS wave function using the determinantal approach, with a maximum number of holes (MxHole) allowed in the RAS1 space and a maximum number of electrons (MxElec) allowed in RAS3 space. In contrast to a FCI or CAS expansion, only a subset of all possible strings should be considered, with a restriction imposed for the maximum number of holes in RAS1 and the maximum number of electrons in RAS3. As a result of such restrictions the string addressing scheme becomes more complicated and is no longer lexical without gaps. In addition to this, not all allowed strings can be combined to obtain determinants.

Let us first consider the addressing scheme for all allowed strings. Let us denote the alpha string as $I_\alpha^{i_h,i_e}$ and the beta string as $I_\beta^{i'_h,i'_e}$. In this representation the number of holes in RAS1 for alpha strings is given by i_h (for beta strings by i'_h), while the number of electrons in RAS3 for alpha strings is given by i_e (for beta strings by i'_e). The total number of α and β active electrons follows from the spin multiplicity and the number of active electrons. The number of α electrons with spin-up in the RAS2 space is the number of active α electrons minus the number of α electrons in the RAS1 and RAS3 subspaces; similarly for β spin.

The above representation of strings allows us to use a two-level addressing scheme. The first level is a string category determined by the number of holes and electrons; the second level gives the local string address within a given category. To demonstrate this, let us define category $\mathrm{Cat}(i_h, i_e)$

$$\mathrm{Cat}(i_h, i_e) = (i_h + 1) + (\mathrm{MxHole} + 1) i_e \ , \tag{2}$$

which assigns a number for a given number of holes i_h and number of electrons i_e. The length of the category is

$$L[\mathrm{Cat}(i_h,\ i_e)] = \binom{\mathrm{RAS1}}{i_h} \binom{\mathrm{RAS2}}{N_\alpha - \mathrm{RAS1} + i_h - i_e} \binom{\mathrm{RAS3}}{i_e} \ , \tag{3}$$

which for a given number of holes and electrons, i_h, and i_e, gives the number of all possible electron distributions in the RAS1, RAS2, and RAS3 spaces. The address of the string can be calculated as

$$\mathrm{Addr}\{I_\alpha^{i_h,i_e}\} = \sum_{i_h,i_e}^{\mathrm{Cat}(i_h,i_e)-1} L[\mathrm{Cat}(i_h, i_e)] + \mathrm{Addr}\{I_\alpha\} \ . \tag{4}$$

The beginning address of each category is precomputed and tabulated. In the above expression the first term gives the sum of lengths of all previous categories, so the first number of the new category gives the number of strings previously accounted for. $\mathrm{Addr}\{I_\alpha\}$ denotes the local string address within a given category. In cases without any restrictions, this addressing scheme becomes identical with the CAS one. The local address can be assigned in the following way: for given i_h and i_e any string can be considered as a superposition of appropriate strings corresponding to electron distributions RAS1, RAS2, and RAS3. To illustrate this let $I(\mathrm{RAS1} - i_h)$, $I(N_\alpha - \mathrm{RAS1} + i_h - i_e)$, and $I(i_e)$ denote the corresponding strings for RAS1, RAS2 and, RAS3 subspaces, respectively. The local address can be now calculated as

$$\begin{aligned}\mathrm{Addr}\{KA\} = \mathrm{Addr}\{I(\mathrm{RAS1} - i_h)\} &+ \binom{\mathrm{RAS2}}{N_\alpha - \mathrm{RAS1} + i_h} \\ &\times [\mathrm{Addr}\{I(N_\alpha - \mathrm{RAS1} + i_h - i_e)\} - 1] \\ &+ \binom{\mathrm{RAS3}}{i_e} (\mathrm{Addr}\{I(i_e)\} - 1) \ ,\end{aligned} \tag{5}$$

consistent with the reversed lexical ordering of string generation. It is convenient to associate a graph to a given category and store all required information for each graph separately. In practice, as was pointed by Olsen et al. [15], only a few graphs are required to generate the set of allowed strings. Note that this is a somewhat different approach from the one presented by Olsen et al. In general we do not impose any restrictions on the graphs; we generate them first as all allowed distributions and finally combine them. Such a graph contains three parts associated with the subspaces of the whole active space. In this approach the head of the graph corresponding to RAS1 becomes the tail of the graph associated with RAS2, while the heads for graphs associated with RAS2 become tails for RAS3. To store all required information for alpha strings one needs (1 + MxHole) (1 + MxElec) such graphs, i.e., nine graphs for MxHole = MxElec = 2.

Each determinant in the RAS expansion can be obtained as a combination of two strings from the allowed list of alpha and beta strings. However, not all strings can be combined freely, because of restrictions for allowed number of holes $(i_h + i'_h) \le \mathrm{MxHole}$ in RAS1 and electrons $(i_e + i'_e) \le \mathrm{MxElec}$ in RAS3. This leads to an addressing array with some gaps; however a two-level addressing scheme can be still applied. Such an extension can be obtained in the following way

$$\begin{aligned}\mathrm{Addr}\{I_\alpha^{i_h,i_e} I_\beta^{i'_h,i'_e}\} &= \sum_{i_h,i_e}^{\mathrm{Cat}(i_h,i_e)-1} \sum_{i'_h,i'_e}^{\mathrm{Cat}(i'_h,i'_e)-1} L[\mathrm{Cat}(i_h, i_e)] \\ &\times L\big[\mathrm{Cat}(i'_h, i'_e)\big] + \mathrm{Addr}\{I_\alpha, I_\beta\} \ ,\end{aligned} \tag{6}$$

where the summation in the last equation is restricted to combinations such that $(i_h + i'_h) \le \mathrm{MxHole}$ and $(i_e + i'_e) \le \mathrm{MxElec}$. Again, in the last equation the first term gives the total number of determinants which were included in previous categories. The second term, $\mathrm{Addr}\{KA,\ KB\}$ gives the local determinant address, which reads

$$\mathrm{Addr}\{I_\alpha, I_\beta\} = \mathrm{Addr}\{I_\alpha\} + L\big[\mathrm{Cat}(i'_h, i'_e)\big]\big(\mathrm{Addr}\{I_\beta\} - 1\big) \tag{7}$$

The beginning address of the various permissible combinations of the $\mathrm{Cat}(i_h, i_e)$ and $\mathrm{Cat}(i_h, i_e)$ categories are also precomputed and stored in a table.

As an example, consider an 18-electron singlet RAS wavefunction with the 18 active orbitals subdivided as (6+6+6), a maximum of two holes in the RAS1 space, and two electrons in RAS3. The 9α and 9β electrons give 8300 strings each, for a total of 1,676,200 determinants. The allowed strings can be divided into nine categories. The α string $I_\alpha^{1,1} = (12346)(246)(3)$ falls into the Cat(1, 1) = 5 category, while the β string $I_\beta^{0,1} = (123456)(35)(4)$ falls into the Cat(0,1) = 4 category. The local address for the first string can be obtained as Addr$\{(12346)\} = 2$, Addr$\{(246)\} = 13$, and Addr$\{(3)\} = 1 + \binom{3-1}{1} = 3$, where the last address calculation is shown in detail. From this Addr$\{I_\alpha\} = 2 + \binom{6}{3}(13-1) + \binom{6}{1}(3-1) = 254$. Similarly, the local address for the beta string is Addr$\{(123456)\} = 1$, Addr$\{(35)\} = 1 + \binom{3-1}{1} + \binom{5-1}{2} = 9$, Addr$\{(4)\} = 4$, which combine to give Addr$\{I_\beta\} = 1 + \binom{6}{2}(9-1) + \binom{6}{1}(4-1) = 139$. The base addresses of the categories (0,0), (1,0), (2,0), (0,1), (1,1), (2,1), (0,2), (1,2), (2,2) are, in this order, 0, 20, 110, 200, 290, 1120, 2470, 2560, 3910. Combining the base addresses with the local address gives Addr$\{I_\alpha^{1,1}\} = 290 + 54 = 544$, Addr$\{I_\beta^{0,1}\} = 200 + 139 = 339$, and Addr$\{I_\alpha^{1,1} I_\beta^{0,1}\} = 487300 + 544 + 90 \times (339-1) = 517720$.

3 Computational implementation

The most computationally demanding part of UNO-RAS calculations is the multiplication of the Hamiltonian matrix by the eigenvector $\mathbf{C}^{(n)}$ in the nth iteration. This is carried out in terms of molecular integrals:

$$\sigma(I_\alpha, I_\beta) = \sum_{J_\alpha J_\beta} \langle J_\beta, J_\alpha | \hat{H} | I_\alpha, I_\beta \rangle C^{(n)}(J_\alpha, J_\beta) \ , \tag{8}$$

The Hamiltonian in CI space can be written in terms of the unitary group generators as

$$\hat{H} = \sum_{i,j} h_{ij} \hat{E}_{ij} + \frac{1}{2} \sum_{i,j,k,l} (ij|kl)(\hat{E}_{ij}\hat{E}_{kl} - \delta_{ik}\hat{E}_{il}) \ , \tag{9}$$

where i, j, k, l label molecular orbitals, h_{ij} and $(ij|kl)$ are one- and two-electron integrals, while the excitation operators $\hat{E}_{ij}$ are the generators of the unitary group $U(n)$

$$\hat{E}_{ij} = \hat{E}_{ij}^\alpha + \hat{E}_{ij}^\alpha \ . \tag{10}$$

Using Eq. (10) and absorbing the second part of the two-electron integral expression into the one-electron integrals

$$g_{ij} = h_{ij} - \frac{1}{2} \sum_n (in|nj) \ , \tag{11}$$

leads to the following expression for the σ vector [17, 22].

$$\sigma(I_\alpha, I_\beta) = \sigma^{(1)}(I_\alpha, I_\beta) + \sigma^{(2)}(I_\alpha, I_\beta) + \sigma^{(3)}(I_\alpha, I_\beta) \ . \tag{12}$$

The $\sigma^{(1)}$ term has the form

$$\sigma^{(1)}(I_\alpha, I_\beta) = \sum_{J_\beta} \sum_{k,l} \langle J_\beta | \hat{E}_{ij}^\beta | I_\beta \rangle \ g_{kl} C(I_\alpha, I_\beta) + \frac{1}{2} \sum_{J_\beta} \sum_{i,j,k,l} \langle J_\beta | \hat{E}_{ij}^\beta \hat{E}_{kl}^\beta | I_\beta \rangle \ (ij|kl) C(I_\alpha, J_\beta) \ , \tag{13}$$

the second term, $\sigma^{(2)}$, reads

$$\sigma^{(2)}(I_\alpha, I_\beta) = \sum_{J_\alpha} \sum_{k,l} \langle J_\alpha | \hat{E}_{ij}^\alpha | I_\alpha \rangle \ g_{kl} C(J_\alpha, I_\beta) + \frac{1}{2} \sum_{J_\alpha} \sum_{i,j,k,l} \langle J_\alpha | \hat{E}_{ij}^\alpha \hat{E}_{kl}^\alpha | I_\alpha \rangle \times (ij|kl) C(J_\alpha, I_\beta) \ , \tag{14}$$

and the expression for $\sigma^{(3)}$ is

$$\sigma^{(3)}(I_\alpha, I_\beta) = \sum_{J_\alpha} \sum_{J_\beta} \sum_{i,j,k,l} \langle J_\alpha | \hat{E}_{ij}^\alpha | I_\alpha \rangle \langle J_\beta | \hat{E}_{kl}^\beta | I_\beta \rangle \times (ij|kl) C(J_\alpha, J_\beta) \ . \tag{15}$$

In our computational implementation of the above equations we use the following strategy. First, we obtain the UHF wave function for the system under consideration. Note that finding solutions of the UHF equations is often not a trivial problem, particularly for systems with an even number of electrons. To accomplish this we use a method based on the theory of triplet instability which is described in Ref. [29]. We then form the first-order density matrix, construct UNOs and check their occupancy. If the occupation is between 0.02 and 1.98 the orbital is considered to be active. To obtain the RAS partition of the active space we check the occupancy of the active orbitals. Orbitals with an occupancy between 0.1 and 1.9 constitute the RAS2 space. Having defined the active space we perform the integral transformation. For a large active space the number of integrals is negligible compared to the number of determinants, and they can usually be stored in core memory. According to restrictions of the number of holes in RAS1 and electrons in RAS3, the dimension of each category is precomputed and stored for alpha strings, beta strings, and for the RAS expansion, respectively. Then we calculate all required alpha strings, $I_\alpha^{i_h,i_e}$, and beta strings $I_\beta^{i_h,i_e}$, and store them according to their given category. For each alpha string we compute all singly excited strings, $\hat{E}_{ij}^\alpha I_\alpha^{i_h,i_e}$, and the same for beta strings, $\hat{E}_{ij}^\beta I_\beta^{i'_h,i'_e}$. If the excitation is out-of-space we reject the string, otherwise we store the address of the excited string together with the numerical value of the coupling coefficient, which is simply ± 1. The combination of two single excitations, which is required for the evaluation of $\sigma^{(1)}$ and $\sigma^{(2)}$, may lead to an excitation which is out-of-space. If singly excited strings are stored according to categories such excitations can simply be eliminated. With suitable string definitions and organization, loop structures for the evaluation of $\sigma^{(1)}$, $\sigma^{(2)}$, and $\sigma^{(3)}$ for the RAS expansion require only minor modification to full CI algorithms, a procedure which is well documented in the literature [15, 17, 19, 22].

It is worth mentioning that for states with $M_s = 0$, the spin-flip symmetry of the coefficient matrix can be used in calculations

$$C(I_\alpha, I_\beta) = (-1)^S C(I_\beta, I_\alpha) \ . \tag{16}$$

As a result of the above relation, only $\sigma^{(1)}$ and part of $\sigma^{(3)}$ have to be generated to obtain the whole σ vector. The determinant-based CI expansion is not spin-adapted

and consequently some roots with higher multiplicity may be found among roots which are sought using Davidson iterative diagonalization [30]. A partial spin adaptation can be obtained using spin-reversal symmetry

$$\Phi = \frac{1}{\sqrt{2}}\left[(I_\alpha, I_\beta) + (I_\beta, I_\alpha)\right] \tag{17}$$

valid for singlet wave functions. The above expansion makes the addressing scheme more complicated; however the length of the RAS expansion is reduced by a factor of almost 2.

4 Comparison between MP2 and UNO occupation criteria

The performance of the RAS (or CAS) method depends critically on the proper selection of the orbital spaces. An alternative criterion, based on second-order Mller-Plesset (MP2) occupation numbers was put forward by Jensen et al. [31]. At first sight, this criterion appears preferable to the (computationally less demanding) UNO criterion. However, we have found that it is less reliable in practice. The reason is that MP2 occupation numbers include the cumulative effect of numerous small correlation contributions while the UNO criterion responds only to a strong correlation by a single correlating orbital (Fig. 1). Thus the MP2 occupation number of a strongly occupied orbital can be quite low without strong nondynamical correlation. For instance, in azulene, a selection criterion based on occupation numbers below 1.952 places two strongly occupied σ orbitals in the active space and omits one $b_1\pi$ orbital. Both chemical intuition and CAS calculations concur that the active space ought to contain the ten π orbitals.

5 Examples: azulene and free base porphyrin

The UNO-RAS method has been implemented and interfaced with the Texas suite of programs for electronic structure calculations. In this section we apply the UNO-CAS and UNO-RAS methods for the ground and excited states of azulene and free base prophyrin.

5.1 Azulene

Azulene is a strongly correlated system with low-lying excited states. We have recently carried out a study of the azulene ground state geometry and vibrations [32] using both UNO-CAS and density functional theory (DFT) with the B3-LYP exchange-correlation potential. We use the DET geometry of the ground state of Ref. [30] in this study. Figure 2 shows the UHF NO occupation histogram. The UNO occupancy criterion for selection of the active space gives ten active orbitals for azulene, essentially a full CI in the valence π space. Four of these orbitals have strong fractional occupancy, pointing to strong nondynamical correlation. This is analogous to the electronic structure of free base porphyrin which will be discussed in Sect. 5.2.

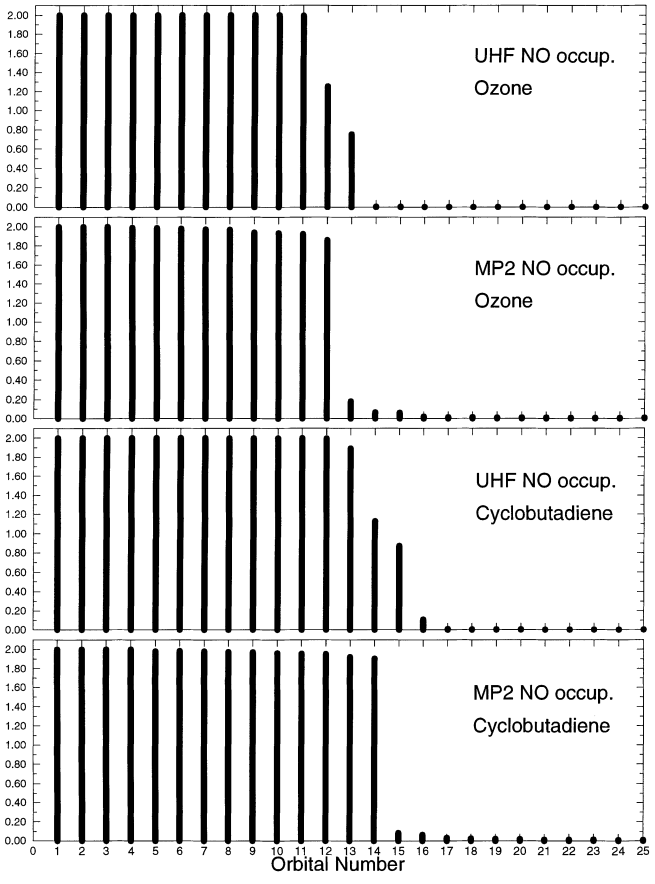

Fig. 1. Comparison of UHF NO and MP2 NO occupation numbers for ozone (two *upper* histograms) and for cyclobutadiene (two *lower* histograms)

CAS-SCF, UNO-CAS, RAS-SCF, and UNO-RAS results are compared for the ground state of azulene in Table 1. Our CAS-SCF and RAS-SCF results were obtained using the Sirius program [33] and our UNO-CAS and UNO-RAS results were obtained with Texas. In both series of calculations we used the same geometry, basis set, and active space. The difference in the CAS-SCF and UNO-CAS energies is only about 1.4 mhartree. This point has been analyzed in previous studies [5]. For our RAS calculations we divided the CAS space of ten active orbitals based on the UNO orbital occupation shown in Fig. 1. The UHF NO occupation histogram clearly shows that among the ten orbitals, which constitute the whole active space, three are more-or-less doubly occupied with occupation numbers of 1.9566, 1.9428, and 1.9265, respectively. Four orbitals (two HOMO and two LUMO) show strong fractional occupancy with occupation numbers of 1.6514 (b_1), 1.6500 (a_2), 0.3500 (a_2), and 0.3486 (b_1). The remaining three orbitals are weakly occupied active orbitals, with 0.0735, 0.0572, and 0.0434 occupation. The most natural splitting of the active space will be RAS1 = 3, RAS2 = 4, and RAS3 = 3. Using this partition we performed calculations with two holes and two electrons allowed in RAS1 and RAS3 space, respectively. In the second expansion we allowed three holes in RAS1 and three electrons in RAS3. To obtain our converged RAS-SCF

[3 + 4 + 3] (2h2e) wave function took almost twice as many iterations as CAS-SCF, while the RAS [3 + 4 + 3] (3h3e) wave function converged poorly and the iterative procedure had to be restarted. The UNO-RAS calculations took only a fraction of the computer time required for RAS-SCF and give an energy only 1.3 and 1.5 mhartree higher. It is difficult to give a definite figure for the savings of UNO-RAS as compared with the RAS-SCF method. For example, one CI iteration for the RAS [3 + 4 + 3] (2h2e) wave function requires about 13 s on a RS/6000 workstation and about 15 iterations to achieve convergence.

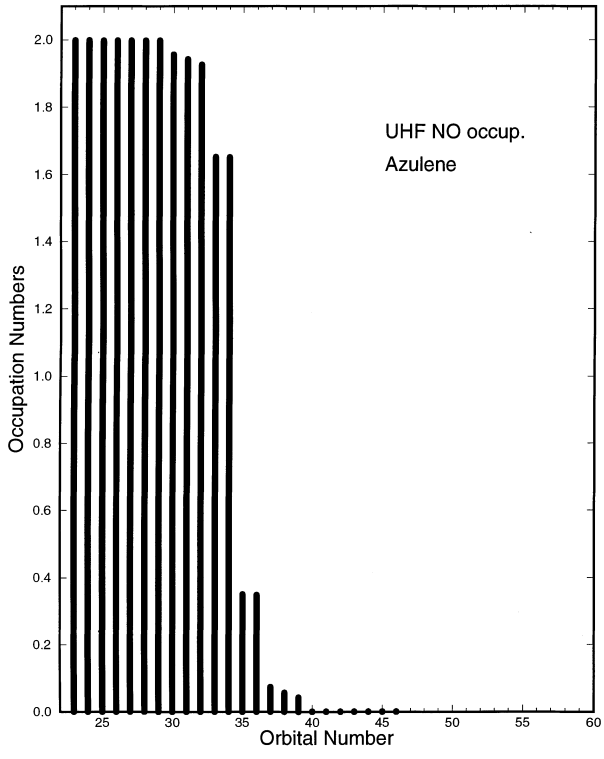

Fig. 2. UHF NO occupation histogram for azulene

Table 1. CAS-SCF, RAS-SCF, UNO-CAS and UNO-RAS energies for azulene[a,b]

	[10elec/10orb][c]	[3 + 4 + 3] (2h2e)[d]	[3 + 4 + 3] (3h3e)[e]
Sirius	CAS-SCF	RAS-SCF	RAS-SCF
	(5 iter)	(11 iter)	(17 iter)[f]
Energy	−383.413 062	−383.407 229	−383.411 924
Texas	UNO-CAS	UNO-RAS	UNO-RAS
Energy	−383.411 638	−383.405 904	−383.410 382

[a] At the DFT/B3-LYP optimized geometry with 6-31G* basis set (Ref. [32])
[b] SCF energy = −383.279 604 (a.u.)
[c] Active space (A_1, A_2, B_1, B_2) = (0, 4, 6, 0)
[d] Active space subdivided into groups of RAS1 = 3, RAS2 = 4, RAS3 = 3 orbitals. Number of holes limited to two in RAS1 and number of electrons limited to two in RAS3
[e] Active space subdivided into groups of RAS1 = 3, RAS2 = 4, RAS3 = 3 orbitals. Number of holes limited to three in RAS1 and number of electrons limited to three in RAS3
[f] Convergence problem

To make a comparison between the UNO-CAS and UNO-RAS methods, we made a cut through the potential energy surface which represents a saddle point for the valence tautomerization of azulene. This corresponds to motion along the $C_s \rightarrow C_{2v} \rightarrow C_s$ coordinate (see Ref. [32] for a detailed discussion). The energy profiles along this path are shown in Fig. 3. The curve for the RAS expansion with three holes in RAS1 and three electrons in RAS3 is almost parallel to the lower one. The upper curve corresponds to the RAS expansion with two holes in RAS1 and two electrons in RAS3. Contrary to the other curves, this curve exhibits only one minimum.

We have calculated vertical excitation energies for azulene using the 6-31G* basis set. This is the first report of the application of the UNO-CAS method to excited states. We must comment, however, that excited states calculated using the ground-state UNO-CAS orbitals are only able to account for low-lying valence-like excited states, and even these are likely to be overestimated as the orbitals are optimized for the ground state. The 6-31G* basis is probably not large enough for describing excited states, particularly the more diffuse ones. The first few transition energies are summarized in Table 2. We also tabulate the QCFF/PI and CIS results of Negri and Zigierski [34]. The experimental data were taken from Ref. [35].

Calculations were carried out with two different UNO-CAS wave functions. The first expansion corresponds to a small active space with four electrons distributed between four orbitals. We performed those calculations only to generate a good starting point for the second UNO-CAS calculation with a large active space. Comparison with experiment shows that vertical excitation energies for the small expansion are overestimated by 2–3 eV. We used results from the small expansion as inputs to the larger calculation using a

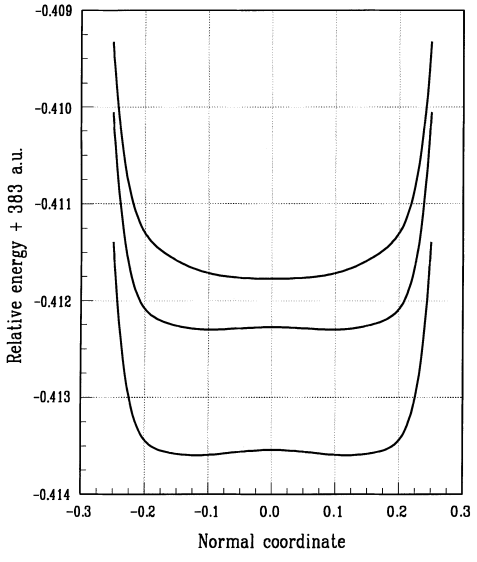

Fig. 3. The energy profiles along the $C_s \rightarrow C_{2v} \rightarrow C_s$ coordinate for azulene. The lower curve corresponds to UNO-CAS calculations, the two upper curves show UNO-RAS [3 + 4 + 3] (3h3e) and UNO-RAS [3 + 4 + 3] (2h2e) calculations, respectively

Table 2. Comparison of the calculated vertical excitation energies (eV) in azulene

State	CAS-SCF [4elec/4orb][a]	UNO-CAS [4elec/4orb][b]	CAS-SCF [10elec/10orb][a]	UNO-CAS [10elec/10orb][b]	QCFF/PI CISD[c]	QCFF/PI CIS[c]	CIS/6-31G[c]	Exprt.[d]
B_2	3.18	4.43	1.95	2.10	1.84	2.15	2.99	1.78
A_1	4.69	5.84	4.42	4.60	3.68	3.41	4.25	3.52
B_2	6.61	7.40	4.57	4.73	3.99	4.31	5.81	4.19
A_1	6.69	7.87	5.47	5.63	4.24	4.68	6.32	4.42

[a] State-averaged CAS with 6-31G* basis set
[b] This work with 6-31G* basis set
[c] From Ref. [34]
[d] From Ref. [35]

starting vector procedure which can be described as follows. First, we generate a small CI expansion and use finite diagonalization to find starting vectors. Then we use a simple mapping procedure between determinants in the two active spaces to generate good initial vectors for the Davidson iterative diagonalization. Results obtained with the large active space agree much better with experimental excitation energies. Comparison of our UNO-CAS results with experimental values shows that agreement for B_2 states is much better than for A_1 states. This probably reflects the fact that the UNO-CAS method has difficulty reproducing excitation energies of ionic excited states, though fairly reliable results are obtained for covalent structures. It is quite clear that the UNO-CAS method is able to take into account the effects of π correlation only, but for those states inclusion of σ electron correlation is crucial. σ correlation can be included by using second-order perturbation theory on top of the UNO-CAS method [2–4]. Table 2 shows that the UNO-CAS results are better than the CIS results with the 6-31G* basis set. However, the fact that the semiempirical QCFF/PI method is more accurate than UNO-CAS is disappointing, and illustrates the difficulty of obtaining accurate ab initio excitation energies.

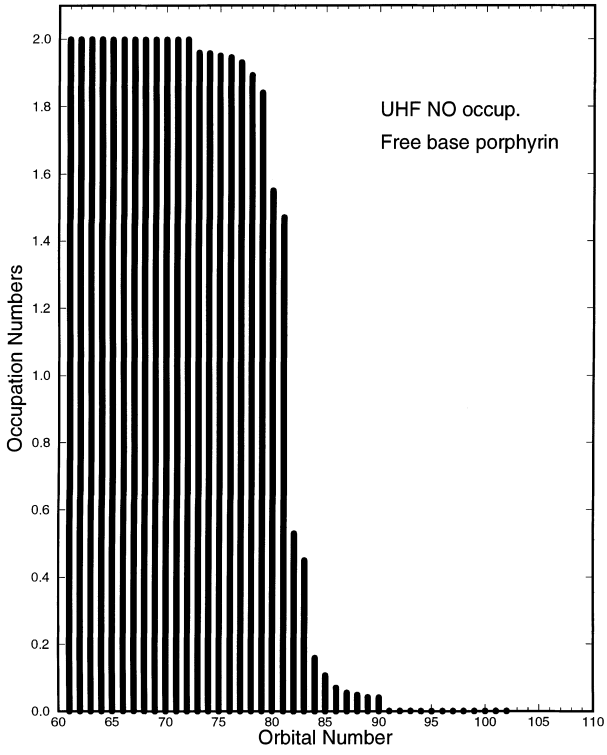

Fig. 4. UHF NO occupation histogram for free base porphyrin

5.2 Free base porphyrin

The second system considered in our study is a free base porphyrin (FBP). Recently, several accurate theoretical studies have been published for this system. Primarily because of its size, earlier calculations on FBP were restricted to low levels of theory. Kozlowski et al. [36–38] have reproduced the FBP vibrational spectrum with remarkable accuracy and have definitely established that the ground state has D_{2h} symmetry using a comparison of experimental vibrational spectra and predictions from hybrid density functional theory. The latest ab initio results for the excited states are those of Merchan et al. [39] using multiconfigurational second-order perturbation theory (CASPT2), the symmetry adapted cluster–configuration interaction (SAC-CI) results of Nakatsuji et al. [40], and similarity-transformed equation-of-motion coupled-cluster singles and doubles (STEOM-CCSD) calculations of Bartlett and coworkers [41].

The geometry used in the present work was obtained in our earlier B3-LYP/6-31G* study [36]. Using the same basis set we calculated the UNO occupancy shown in Fig. 4. Using the usual UNO occupancy criterion (i.e., between 2-x and x, x being equal to 0.02) to select the active space leads to 18 active orbitals. The active space contains four partially occupied orbitals with occupancy 1.5498 (a_u), 1.4697 (b_{3u}), 0.5303 (b_{2g}) and 0.4502 (b_{1g}). The importance of those four frontier orbitals was recognized by Gouterman [42] a long time before any ab initio calculations. This definition of the active space is different to the one Merchan et al. use in their RAS-SCF calculations [43]. These authors used the full valence active space to define the RAS-SCF wave function (22 π active orbitals, 22 π active electrons). The UNO occupation criterion leads to only 18 active orbitals, which characterize the principal resonance structures of FBP, an 18-membered cyclic polyene ring (see, for example, Fig. 1, Ref. [37]).

We have calculated excitation energies using different UNO-CAS and UNO-RAS expansions. Our results are summarized in Table 3. For completeness we also include CIS, CASPT2, and SCA-CI results. Experimental excitation energies were taken from Ref. [44]. Initially,

Table 3. Comparison of the calculated vertical excitation energies (eV) for free base porphyrin

State	CAS-SCF [4elec/4orb][a,b]	UNO-CAS [4elec/4orb][c]	UNO-CAS [12elec/12orb][c]	UNO-RAS [7+4+7] (2h 2e)[c,d]	CIS[e]	CASPT2[f]	SAC-CI[g]	STEOM-CC[h]	Expt.[i]
1^1B_{1u} (Q_x)	3.56, 3.44	3.69	2.57	2.44	2.77	1.33	1.80	1.72	1.98
1^1B_{2u} (Q_y)	3.82, 3.66	4.26	4.01	4.28	3.15	2.05	2.25	2.61	2.42
2^1B_{1u} (B_x)	5.14, 5.45	5.81	5.24	5.08	5.04	2.98	3.59	3.63	3.33
2^1B_{2u} (B_y)	5.17, 5.48	6.00	5.48	5.12	5.71	3.08	3.79	3.77	3.33

[a,b] Ref. [39] with ANO-type C, N[3*s*2*p*]/H[1s] basis set, state-averaged CAS with C,N VDZP/H, VDZ basis set
[c] This work
[d] Active space subdivided into groups of RAS1 = 7, RAS2 = 4, RAS3 = 7 orbitals. Number of holes limited to two in RAS1 and number of electrons limited to two in RAS3
[e] Ref. [45]
[f] Ref. [39]
[g] Ref. [40]
[h] Ref. [41]
[i] Ref. [44]

we performed our calculations with four active orbitals (HOMO, HOMO-1, LUMO, LUMO-1) and four active electrons (Gouterman's four orbital model). Our results are not significantly different from the CAS-SCF (4/4) results of Merchan et al. [39]. Their excitation energies are 3.99, 4.56, 5.76, and 5.87 eV while ours are 3.69, 4.26, 5.81, and 6.00 eV. In addition, we performed two other calculations. In the first we used a UNO-CAS expansion with 12 active orbitals and 12 active electrons. The difference between the calculated and experimental vertical excitations is reduced, although the average difference is still about 2 eV. In our final calculations we used a UNO-RAS expansion, with an active space subdivided into groups of RAS1 = 7, RAS2 = 4, and RAS3 = 7 orbitals. We limited the number of holes in RAS1 and the number of electrons in RAS3 to two. Although the results obtained with the larger UNO-RAS space improve somewhat compared to smaller active spaces, they are still significantly (up to 1.75 eV) in error. This shows that CAS-type wave functions with limited active spaces, without the inclusion of dynamical electron correlation, are insufficient for the calculation of accurate excitation energies, a conclusion also supported by results from other groups.

6 Conclusions

We have developed an efficient implementation of the UNO-RAS method. This method uses the inexpensive UHF NOs in a RAS expansion. The assignment of the orbitals to three RAS subspaces is governed by the occupation number of the UHF Nos. We discuss the addressing scheme for the most efficient calculation of the CI wavefunction in the restricted active space. Applications to the ground and lower excited states of azulene and FBP are presented. In spite of the large active space which the UNO-RAS method allows, the excitation energies for FBP are still significantly in error, pointing to the necessity of including dynamical correlation effects. Even though the absolute excitation energies are not very accurate, there is hope that the overall shape of the excited state energy surfaces are at least qualitatively correct. This would allow, for example the prediction of resonance Raman intensities.

Acknowledgements. We would like to thank Dr. Hans Jorgen Aa. Jensen from the University of Odense, Denmark for providing us with a copy of the Sirius program. This study has been supported by the National Science Foundation under grant no. CHE-9319929.

References

1. Werner H-J (1987) Adv Chem Phys 69: 1; (b) Shepard R *ibid*, 69: 63; (c) Roos BO *ibid*. 69: 399
2. Wolinski K, Pulay P (1989) J Chem Phys 90: 3647
3. (a) Anderson K, Malmqvist P-A, Roos BO, Sadlej AJ, Wolinski K (1990) J Phys Chem 94: 5483; (b) Anderson K, Malmqvist P-A, Roos BO (1992) J Chem Phys 96: 1218
4. Kozlowski PM, Davidson ER (1994) J Chem Phys 100: 3672
5. Bofill JM, Pulay P (1989) J Chem Phys 90: 3637
6. Pulay P, Hamilton T (1988) J Chem Phys 88: 4926
7. Chipman D, Liu R, Zhou X, Pulay P (1994) J Chem Phys 100: 5023
8. Pulay P, Bofill JM (1989) Chem Phys Lett 156: 501
9. Liu R, Pulay P (1992) J Comput Chem 13: 193
10. Liu R, Zhou X, Pulay P (1992) J Phys Chem 96: 5748
11. Liu R, Pulay P (1992) J Chem Phys 97: 1602
12. Liu R, Zhou X, Pulay P (1992) J Phys Chem 96: 4255
13. Fogarasi G, Liu R, Pulay P (1993) J Phys Chem 97: 4036
14. Bone RGA, Pulay P (1993) In J Quantum Chem 45: 133
15. Olsen J, Roos BO, Jorgensen P, Jensen HJAa (1988) J Chem Phys 89: 2185
16. Knowles PJ, Handy NC (1984) Chem Phys Lett 111: 315
17. Zarrabian S, Sarma CR, Paldus J (1989) Chem Phys Lett 155: 183
18. Knowles PJ Chem Phys Lett (1989) 155: 513
19. Harrison RJ, Zarrabian S (1989) Chem Phys Lett 158: 393
20. Knowles PJ, Handy NC (1989) J Chem Phys 91: 2396
21. Bauschlicher CW Jr, Langhoff SR, Taylor PR (1990) Adv Chem Phys 77: 103
22. Olsen J, Jorgensen P, Simons J (1990) Chem Phys Lett 169: 463
23. Harrison RJ (1991) J Chem Phys 94: 5021
24. Luzanov AV, Wulfov AL, Krouglov VO (1992) Chem Phys Lett 197: 614
25. Bendazzoli GL, Evangelist S (1993) J Chem Phys 98: 3141
26. Bendazzoli GL, Evangelisti S (1993) Int J Quantum Chem Symp 27: 287
27. Mitrushenkow AO (1994) Chem Phys Lett 217: 559
28. Duch W (1986) GRMS or graphical representation of model space. Springer, Berlin Heidelberg New York

29. Pulay P, Liu R (1990) J Phys Chem 94: 5548
30. Davidson ER (1975) J Comput Phys 17: 87
31. Jensen HJAa, Jorgensen P, Argen H, Olsen J (1988) J Chem Phys 88: 3834; (1998) J Chem Phys 88: 5354
32. Kozlowski PM, Rauhut G, Pulay P (1995) J Chem Phys 103: 5650
33. Sirius is a direct, restricted-step second-order MCSCF program
34. Negri F, Zgierski MZ (1995) J Chem Phys 99: 4318
35. Dekkers HPJM, Westra SWT (1975) Mol Phys 30: 1795
36. Kozlowski PM, Zgierski MZ, Pulay P (1995) Chem Phys Lett 247: 379
37. Kozlowski PM, Jarzecki AA, Pulay P (1996) J Phys Chem 100: 7007
38. Kozlowski PM, Jarzecki AA, Pulay P, Li X-Y, Zgierski MZ (1996) J Phys Chem 100: 13985
39. Merchan M, Orti E, Roos BO (1994) Chem Phys Lett 226: 27
40. (a) Nakatsuji H, Hasegawa J, Hada M (1996) J Chem Phys 104: 2321; (b) Tokita Y, Hasegawa J, Nakatsuji H (1998) J Phys Chem A 102: 1843
41. (a) Nooijen M, Bartlett RJ (1997) J Chem Phys 106: 6449; (b) Gwaltney SR, Bartlett RJ (1998) J Chem Phys 108: 6790
42. Gouterman M (1978) In: Dolphin D. (ed) The porphyrins, vol III, part A. Academic Press, New York, pp 1–156
43. Merchan M, Orti E, Roos BO (1994) Chem Phys Lett 221: 136
44. Edwards L, Dolphin DH (1971) J Mol Spectrosc 38: 16
45. Foresman JB, Head-Gordon M, Pople JA, Frisch MJ (1992) J Phys Chem 96: 135